encit 2020

ABCM Associação Brasileira de Engenharia e Ciências Mecânicas

18th Brazilian Congress of Thermal Sciences and Engineering
November 16-20, 2020 (Online)

ENC-2020-0917
Optimization of Hydrofoil by Genetic Algorithm

Vinícius Gomes Pereira Siston[1]
Guilherme Amaral do Prado Campos[1,2]
João Victor Barros dos Santos[1]
Luciano Santos Constantin Raptopoulos[1]
Max Suell Dutra[2]

[1]Centro Federal de Educação Tecnológica Celso Suckow da Fonseca campus Nova Iguaçu - Departamento de Engenharia Mecânica, Estrada de Adrianópolis, n°1.317, Santa Rita, Nova Iguaçu, RJ, CEP 26041-271, Brazil

[2]Universidade Federal do Rio de Janeiro-UFRJ - Centro de Tecnologia, Cidade Universitária, Av Horácio Macedo n°2030, Rio de Janeiro, RJ, 21941-914, Brazil

viniciusgpsiston1@gmail.com, guilherme.campos@cefet-rj.br, joaovictor.96@hotmail.com, luciano.raptopoulos@cefet-rj.br and max@mecanica.coppe.ufrj.br

Abstract. *More evident local or global environmental problems increase the demand for renewable energy sources, such as ocean currents. In this paper, the shape of an oscillating hydrofoil is optimized to make the energy generating device more efficient, increasing the lift coefficient and lift-to-drag ratio, and to preventing cavitation. Multi-objective optimization is done through the agglutination technique and using a different application of the Genetic Algorithm (GA), where different percentages of the leading and trailing edges of a set of NACA profiles are combined for the crossover phase. The proposed optimization method proved to be effective for the case of the lift coefficient.*

Keywords: *optimization, genetic algorithm, flapping foil*

1. INTRODUCTION

Renewable energies for most of human history have been the main or the only option available. The use of non-renewable sources gained prominence only a few centuries ago. However, local or global environmental problems become increasingly evident, thus reviving the importance of renewable energies (Sørensen, 1991), such as ocean currents.

The conversion of energy from the currents can be done through oscillating hydrofoils, also called flapping foils. In the Fig. 1a it is possible to visualize the flapping foil device that will be used in this work. It is a pair of swinging arms, and at the end of the arms there is a symmetrical hydrofoil. The set has a total of two degrees of freedom and this configuration results in a movement pattern for the hydrofoil represented in Fig. 1b, setting the movement pattern of "Swing Arm", according to Karbasian *et al.* (2016). The symmetrical wing shape gives the device the same behavior both up and down.

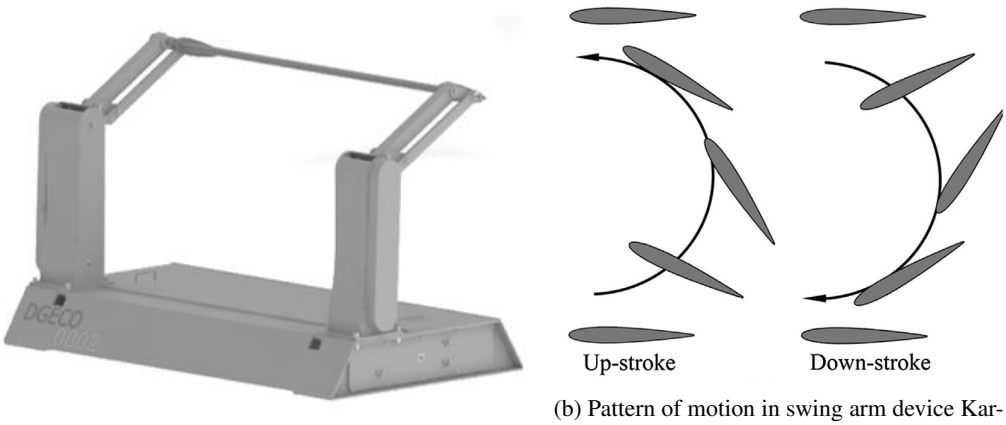

(a) Proposed Project by Campos (2013).

(b) Pattern of motion in swing arm device Karbasian *et al.* (2016).

Figure 1: Details of Flapping Foil.

To improve the use of the energy available in the currents by the flapping foil, it is necessary to optimize the shape of the wing used in the mechanism to obtain better lift coefficients without compromising the lift/drag efficiency.

Due to similarities in operating principle, much of the technology and design theory applied to hydrofoils derives from

the airfoil industry (Elghali *et al.*, 2007; Wang *et al.*, 2018). However, some differences need to be taken into account in hydrodynamic projects, such as the possibility of cavitation by the fluid being incompressible (Gaden, 2007; Batten *et al.*, 2006; Wang *et al.*, 2018). In the case of submerged turbines, for example, pressure fields close to vapor pressure can cause blade erosion and loss of power (Bahaj *et al.*, 2007; Silva *et al.*, 2015). In the Equation 1, the cavitation number σ is defined as,

$$\sigma = \frac{P_{atm} + \rho g h - P_v}{\frac{1}{2}\rho v^2} \tag{1}$$

where: P_{atm} is the atmospheric pressure, ρ is the specific mass of the fluid, g the acceleration of gravity, h the depth, and P_v the vapor pressure of the fluid and v is the velocity of the fluid.

If the minimum negative pressure coefficient ($-C_p$) at any location on the wing is higher than the number of cavitation σ, cavitation will occur (Goundar and Ahmed, 2013; Tahani *et al.*, 2015; Batten *et al.*, 2006). In this paper, the pressure coefficient distribution graph is obtained by simulation. The mathematical relationship of the C_p pressure coefficient, considering the height, can be seen in Equation 2.

$$C_p = \frac{P_l - P_0}{\frac{1}{2}\rho v^2} \tag{2}$$

Where P_l is the local pressure of a point on the surface of the wing and P_0 is the free stream pressure. Cavitation inception can be predicted from the pressure distribution since cavitation will occur when $P_L = P_V$ (Batten *et al.*, 2006).

It is observed that in Equations 1 and 2 speed has a significant influence. According to Wang *et al.* (2018), at low speeds the occurrence of cavitation is negligible. However, it is necessary to determine the limit speed for the occurrence of this phenomenon. If the desired design speed is higher than the cavitation speed, then improvements or adjustments are necessary to achieve the design speed (Zeng and Kuiper, 2012).

Regardless of the possibility of cavitation or not, there are two approaches to profile design: inverse design or direct numerical optimization. The inverse design produces a geometry that satisfies a preset pressure distribution. Direct numerical optimization adds the definition of geometry with aerodynamic analysis which, in an iterative process subject to restrictions, produces optimized designs (Song and Keane, 2004; Della Vecchia *et al.*, 2014; Anitha *et al.*, 2018).

Usually the profile optimization model, in the direct numerical optimization way, consists of using a technique to represent and generate profiles, a profile simulation software, where it is possible to check the characteristics of the profile in working order given the geometry, and a strategy optimization (Zeng and Kuiper, 2012).

In the paper, for the representation of profiles, the Spline interpolation technique is used (De Boor *et al.*, 1978) and the XFOIL code to obtain the data of hydrodynamics characteristics. Drela and Youngren (2001) developed a code based on the boundary element method incorporating of the boundary layer computations (De Boor *et al.*, 1978; Drela, 1989). The optimization method used is the genetic algorithm and its application was discussed in Section 2.

Genetic algorithms (GA) are based on Charles Darwin's theory of species evolution. Individuals better adapted to the environment are more likely to reproduce and pass on their characteristics to their descendants. It is also a robust and accurate method for optimizing global aerodynamic formats and, therefore, it is frequently studied in the literature (Marco and Lanteri, 2000; Wang *et al.*, 2002; Quagliarella and Cioppa, 1995; Mukesh *et al.*, 2014).

2. METHODOLOGY

The profile optimization is done through a genetic algorithm developed with the objectives of maximizing the lift coefficient (C_L) and maximizing the efficiency given by the lift-to-drag ratio (C_L/C_D), meeting the specifications of the power generation device present in Campos *et al.* (2019), seen in Tab. 1.

Table 1: Optmization constraints.

Parameter	**Reynolds**	**Mach**	**Fluid**	**Profile Type**
Value	$4.9 \cdot 10^5$	0.0059	Water	Symmetric

For the multi-objective optimization of the hydrofoil, the agglutination technique is used, consisting of previous simple optimizations to obtain the new evaluation function parameters. The flowchart of hydrofoil optimization can be seen in Fig. 2. The new evaluation function is given by Eq. 3,

$$\phi = -\frac{(C_L)_{max} - C_L}{(C_L)_{max}} - \frac{(C_L/C_D)_{max} - C_L/C_D}{(C_L/C_D)_{max}} \tag{3}$$

where: ϕ is the evaluation function to be minimized, $(C_L)_{max}$ is the maximum value of lift coefficient obtained by optimizing only C_L, C_L is the lift coefficient of the hydrofoil being currently evaluated, $(C_L/C_D)_{max}$ is the maximum value of lift to drag ratio obtained by optimizing only C_L/C_D and C_L/C_D is the lift/drag efficiency of the hydrofoil being evaluated at the time.

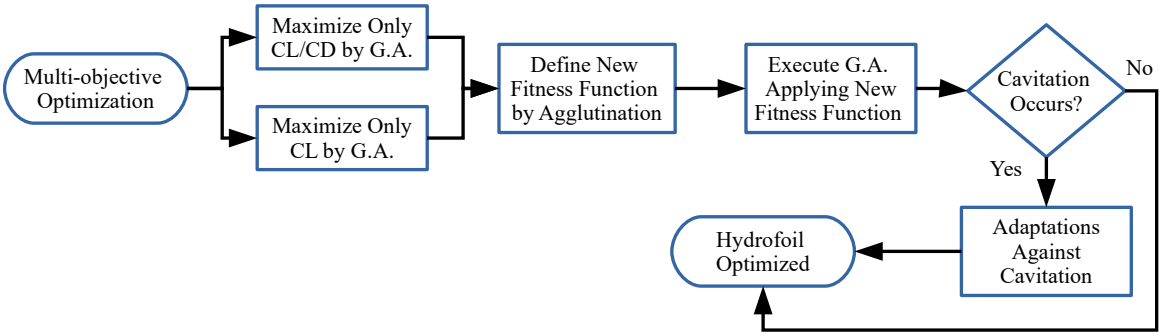

Figure 2: Multi-objective Optimization.

The genetic algorithm flowchart is represented in Figure3.

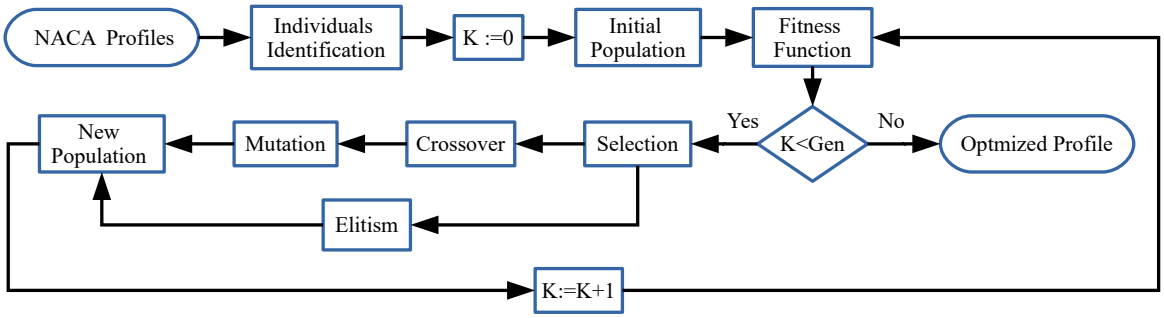

Figure 3: Genetic Algorithm.

From the studies carried out by Campos *et al.* (2019) on an ocillating hydrofoil, it was noticed that a group of profiles stands out in this application: symmetric NACAs. Therefore, this group of hydrofoils was chosen as the initial population of the genetic algorithm. NACA profiles are generated from the function obtained by Abbott and Von Doenhoff (2012) with 199 points. Each profile of the original population is identified. Thus, it is checked which part of the profile has spread to the optimized profile.

The fitness phase is carried out using a function called "XFOIL" widely used in profile studies and uses the panel method to determine, among other things, the C_L, the C_D of a profile for a range of requested angles of attack (α). It is necessary to specify the two-dimensional points that constitute the profile's shape, the number of Reynolds that characterize the flow.

The selection consists of separating the best individuals resulting from the evaluation phase. As the number of individuals between generations remains constant, and the crossing phase is carried out two by two allowing the crossing of all against all those selected, the number of selected individuals must be the square root of the total number of individuals in the population. It implies that the number of individuals must have an entire square root.

The crossing step is done by combining a percentage of one profile's leading-edge with a percentage of the trailing edge of another profile. The "spline" technique interpolates the part of the generated profile with no point in the original profiles (between the leading and trailing edges).

The interpolation performed produces the mutation. The percentages of the leading and trailing edges are generated randomly at each intersection but limited always to allow a minimum of 10% of each original edge. It ensures that there will be a match. Elitism takes the individuals selected for the next generation. This cycle is repeated until the stop criterion is reached. The stopping criterion used is the number of generations "Gen". An example of the result of crossing and mutation can be seen in Fig. 4. It can be seen that in Fig. 4a the crossing occurs between 20% of the leading edge of NACA0020 with 30% of the trailing edge of NACA0010 resulting in MODIFIED A. It is noted that, despite both profiles, NACA0020 and MODIFIED B, have 20% leading edge of NACA0020 and 20% trailing edge of NACA0010, their formats are different.

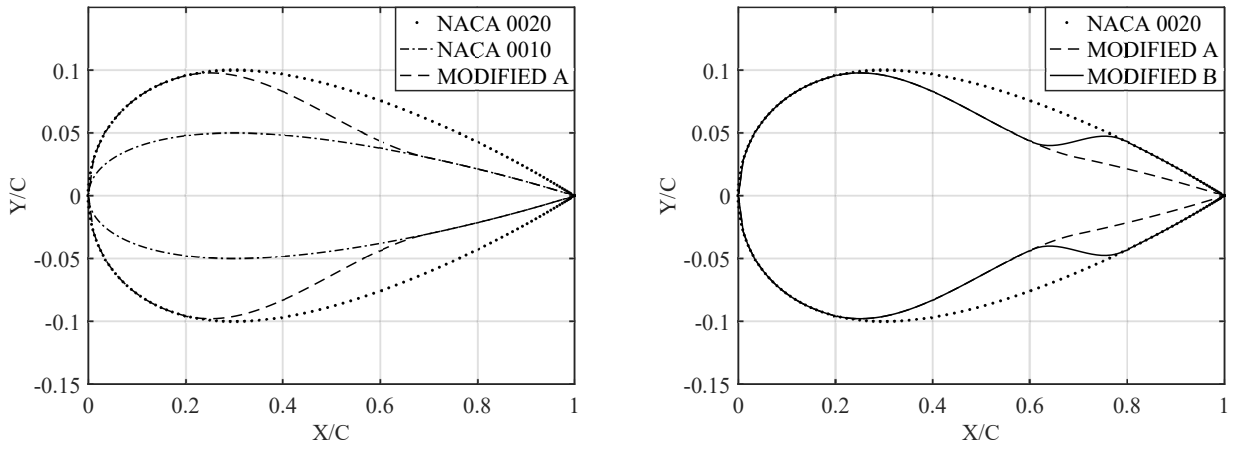

(a) Example between NACA0020 and NACA0010. (b) Example between NACA0020 and MODIFIED A.

Figure 4: Examples of Crossover and Mutation.

3. RESULTS AND DISCUSSION

In this Section, the results of optimization of the lift coefficient (C_L), lift-to-drag coefficient (C_L/C_D) and the agglutination optimization are presented for profile NACA0015. Furthermore, the cavitation was also assessed.

3.1 CL optimization

For the realization of C_L optimization, 15 tests were carried out, separated into 3 groups, each group has a different number of generations, indicated by the number that starts the test name. The execution of tests with different limit numbers of generations aims to verify when convergence occurs and to determine the ideal number of generations, which should always be greater than the generation of convergence.

Table 2: CL Tests Results.

Tests	$(C_L)_{max}$ **[-]**	α-$(C_L)_{max}$ **[deg]**	$(C_L/C_D)_{max}$ - $(C_L)_{max}$ **[-]**	$(C_L/C_D)_{max}$ **[-]**	α - $(C_L/C_D)_{max}$ **[deg]**	**Convergence Generation**	ϕ
5A	1.60	15.50	59.40	66.70	15.00	5	-0.74
5B	1.62	16.25	58.13	67.14	15.00	3	-0.73
5C	1.59	16.00	60.26	70.18	13.75	3	-0.74
5D	1.56	15.25	63.09	69.88	14.50	4	-0.75
5E	1.62	16.00	58.15	58.15	16.00	5	-0.74
10A	1.64	15.50	66.83	70.10	14.75	8	-0.68
10B	1.60	15.25	65.48	72.60	14.00	3	-0.72
10C	1.60	15.25	67.55	71.33	14.75	5	-0.71
10D	1.63	16.25	60.53	65.69	15.25	4	-0.72
10E	1.60	15.75	59.69	61.23	14.75	3	-0.74
15A	1.60	15.50	63.65	71.17	13.75	5	-0.72
15B	1.60	15.50	62.90	69,81	14,50	5	-0.72
15C	1.60	15.50	61.16	67.54	15.00	5	-0.73
15D	1.60	15.50	63.90	68.86	14.75	4	-0.72
15E	1.56	15.00	65.79	74.09	13.75	5	-0.73
AV	1.60	15.60	62.43	68.30	14.63	4.47	-0.73
SD	0.02	0.38	3.09	4.19	0.63	1.30	0.02

The results of the C_L optimization tests can be seen in Tab. 2, as well as means and standard deviations of each parameter. It is noted that in the group of 5 generations, tests 5A and 5E obtained a generation of convergence equal to the limit generation of 5, which means that these tests may not have fully evolved. Although the average generation of convergence between all tests is 4.47, its standard deviation of 1.30 indicates that a category above the group of tests

should be preferred, ie 10 generations. The largest generation of convergence was the 8th obtained in the 10A test, indicating that the ideal number of generations should be greater than 8. In the 10 and 15 generation tests, all tests have developed completely.

It is observed that there is essentially a trade-off between the maximum lift coefficient ($(C_L)_{max}$) that the hydrofoil can develop and the efficiency developed at this operation point ($(C_L/C_D)_{max}$ - $(C_L)_{max}$). Despite this, the 10A test got the best $(C_L)_{max}$ and also got the second best result of $(C_L/C_D)_{max}$ - $(C_L)_{max}$. O $(C_L)_{max}$. The $(C_L)_{max}$ of the 10A test will be used as a parameter in Eq. 3 to perform the optimization by agglutination.

Identification of the original wings allows to track that initial 11% of the leading edge is NACA0023 original and the final 10% of the trailing edge is from NACA0023 also, the remainder is a consequence of crossings and mutation.

The low standard deviation of the parameter $(C_L)_{max}$, SD = 0.02, points to the consistency of the genetic algorithm with 9 of the 15 tests exactly equal to the average of 1.60.

The value of the ϕ function obtained for each test when applying the Eq. 3 can also be seen in Tab. 2. The higher the value, the closer to the optimal profile when considering agglutination. In this indicator, the 10A test was also the best among the other C_L optimization tests.

3.2 CL/CD optimization

For the realization of the C_L/C_D optimization, 15 tests were performed separated into 3 groups, in the same way as the C_L optimization, looking for the ideal number of generations for a test, which should always be greater than the convergence generation.

In Table 3 the results of the C_L/C_D optimization tests can be seen in addition to the means and standard deviations of each parameter. In the groups of 5 10 generations, 3 tests, 5J, 10F and 10G, reached the convergence only in the last generation indicating that the number of generations must be greater. Although the average generation of convergence between the tests is 7.4, where 10-generation tests would meet, its standard deviation of 4.32 points to the need to move up to the 15-generation category. The highest generation of convergence was obtained in the 15G and 15H tests and occurred in the $14th$ generation, thus determining that tests with 15 generations are sufficient for convergence.

Table 3: CL/CD Tests Results.

Tests	$(C_L)_{max}$ **[-]**	α-$(C_L)_{max}$ **[deg]**	$(C_L/C_D)_{max}$ - $(C_L)_{max}$ **[-]**	$(C_L/C_D)_{max}$ **[-]**	α - $(C_L/C_D)_{max}$ **[deg]**	**Convergence Generation**	ϕ
5F	1.22	11.25	78.17	78.17	11.25	3	-0.89
5G	1.26	13.00	114.56	116.09	12.75	3	-0.69
5H	1.18	11.50	97.31	150.54	10.50	1	-0.82
5I	1.30	11.00	80.91	80.91	11.00	4	-0.83
5J	1.50	14.00	76.25	79.09	13.50	5	-0.72
10F	1.29	11.00	79.54	80.53	10.75	10	-0.84
10G	1.30	11.50	81.47	81.90	11.25	10	-0.82
10H	1.36	14.25	123.07	129.84	13.75	2	-0.59
10I	1.31	12.50	210.87	218.21	12.25	8	-0.20
10J	1.30	12.00	79.48	79.48	12.00	7	-0.83
15F	1.30	11.00	79.47	79.47	11.00	12	-0.83
15G	1.40	12.75	80.61	80.61	12.75	14	-0.77
15H	1.38	12.00	80.49	80.86	11.75	14	-0.78
15I	1.31	13.25	170.74	170.74	13.25	11	-0.39
15J	1.22	14.25	82.97	82.97	14.25	7	-0.86
AV	1.31	12.35	101.06	105.96	12.13	7.4	-0.72
SD	0.08	1.19	39.72	43.10	1.19	4.32	0.19

The trade-off between $(C_L)_{max}$ and $(C_L/C_D)_{max}$ - $(C_L)_{max}$, already observed in the C_L optimization tests, it can also be established in the C_L/C_D optimization, especially when comparing the CL optimization means with the C_L/C_D optimization means. In the 10I test, the best efficiency was obtained $(C_L/C_D)_{max}$ - $(C_L)_{max}$ = 210.87, although its $(C_L)_{max}$ is not the smallest.

The 10I test stands out for being about 3 standard deviations above the average efficiency. A possible cause for this is the occurrence of a very specific mutation. Even that, The $(C_L/C_D)_{max}$ - $(C_L)_{max}$ of test 10I will be used as a parameter in Eq. 3 to perform of agglutination optimization.

The average value of ϕ of the C_L/C_D optimization tests was approximately the same as the average of the C_L tests, this points to the expected symmetry trend in the commitment relationship between C_L and C_L/C_D.

Identification of the original wings allows to track that initial 11% of the attack lip is NACA0012 original and the final 18% of the trailing edge is from NACA0023, the remainder is a consequence of crossings and mutation.

The 10I test of best performance in the target parameter of this optimization, C_L/C_D, was also the best in the global parameter among its peers. This test differs from the others by being about 3 standard deviations away from the average in this regard.

3.3 Agglutination optimization

In this optimization, the best C_L parameter of the optimization referring to the Subsection 3.1 and the best C_L/C_D parameter of the optimization referring to the Subection 3.2 were used to build the evaluation function ϕ of Eq. 3. In Table 4 the results are displayed.

Similar to the other optimizations, 15 tests were carried out in groups of 5 with different limit generation to find the most appropriate number of generations. The average number for the generation of convergence in the value of 5.93 and the standard deviation of 3.41 indicate that the category of 10 generations would be more suitable, however the tests 15L, 15N and 15O converged in a number greater than 10 generations. As the largest generation of convergence was the 13th, the total number of generations must be greater than that, so the category of 15 generations is suggested.

Identification of the original wings allows to track that initial 12% of the attack lip is NACA0012 original and the final 17% of the trailing edge is from NACA0023, the remainder is a consequence of crossings and mutation.

In addition, the two best tests were configured in 15 generations. Tests 15L and 15O obtained the best value of $\phi = -0.36$ within this optimization.

The average value of the ϕ value was better in the agglutination than in the other two optimizations, indicating that on average the agglutination proved to be efficient. However, the 10I test was better evaluated globally in the parameter ϕ. The random factor, characteristic of optimization by genetic algorithm, proved to be decisive.

Table 4: Agglutination Tests Results.

Tests	$(C_L)_{max}$ **[-]**	α-$(C_L)_{max}$ **[deg]**	$(C_L/C_D)_{max}$ - $(C_L)_{max}$ **[-]**	$(C_L/C_D)_{max}$ **[-]**	α - $(C_L/C_D)_{max}$ **[deg]**	**Convergence Generation**	ϕ
5K	1.40	13.50	146.39	146.39	13.50	4	-0.45
5L	1.54	14.25	75.01	76.28	14.00	5	-0.70
5M	1.40	13.75	150.06	150.06	13.75	5	-0.43
5N	1.57	15.00	68.77	74.98	13.75	3	-0.72
5O	1.50	14.00	76.02	78.24	13.50	5	-0.72
10K	1.50	14.00	76.73	78.44	13.50	5	-0.72
10L	1.42	15.25	120.08	130.20	14.75	4	-0.56
10M	1.56	14.75	70.52	76.43	13.50	3	-0.71
10N	1.33	13.00	156.37	156.37	13.00	4	-0.45
10O	1.43	13.75	159.20	170.69	13.50	5	-0.37
15K	1.57	14.75	72.83	75.74	14.00	5	-0.69
15L	1.49	14.25	153.00	164.97	13.25	13	-0.36
15M	1.42	15.25	120.08	130.20	14.75	4	-0.56
15N	1.40	13.50	149.40	149.40	13.50	11	-0.44
15O	1.49	14.25	153.00	164.97	13.25	13	-0.36
AV	1.47	14.22	116.50	121.56	13.70	5.93	-0.55
SD	0.07	0.67	38.22	39.50	0.50	3.41	0.15

In Figure 5a the study of convergence of the best agglutination tests can be seen. The initial population of the 15 NACA profiles is assessed at zero generation. It is possible to infer that the 5M test may not have developed completely, since in the last generation it has not yet reached its asymptote. The 10O test reached its maximum value of -0.37 in generation 5 and has not progressed further. The 15L and 15O tests had the same evolution history even though they were independent and converged to the best value in generation 13.

The parameters of the 45 tests performed on a graph of $(C_L)_{max}$ for C_D is presented in the Fig. 5b. It is observed that the C_L tests are grouped in the region of the graph that denotes high $(C_L)_{max}$ and high CD. The C_L/C_D tests populate the region of the low $(C_L)_{max}$ and low C_D in the chart. The agglutination tests, although dispersed, are in an intermediate

area of the graph. In this graph, the best individuals are those who managed to establish their parameters at the border where the $(C_L)_{max}$ is high and at the same time the C_D is high, according to the criterion of the ϕ function, while the worst are in the opposite direction on the graph.

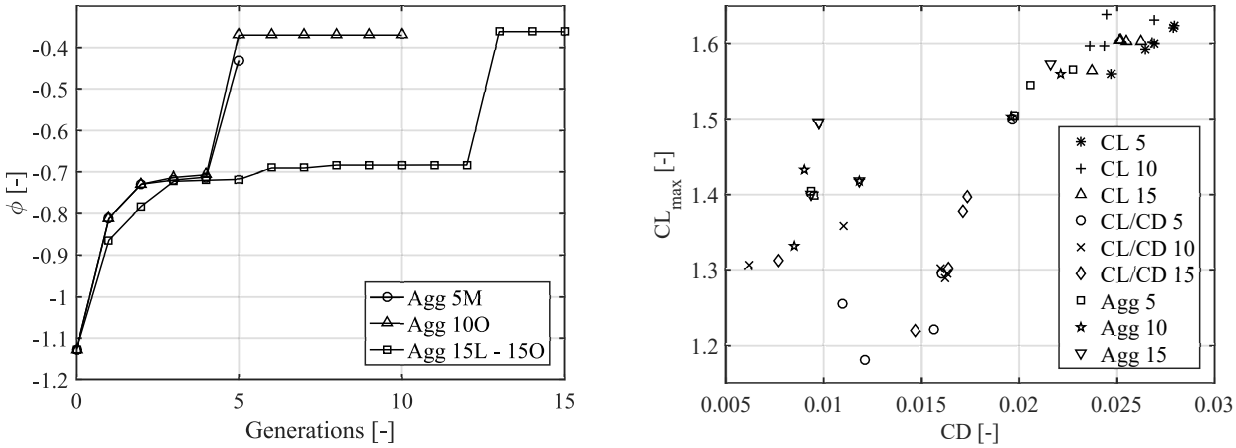

(a) Convergence study. (b) Pareto's curve.

Figure 5: Convergence study and Pareto's curve.

In order to compare the profiles obtained in this work with the NACA0015 profile currently used, the values of the evaluation are displayed in the Tab. 5. The value of ϕ is the worst among all tests performed.

Table 5: NACA0015 test results.

Test	$(C_L)_{max}$ **[-]**	α-$(C_L)_{max}$ **[deg]**	$(C_L/C_D)_{max}$ - $(C_L)_{max}$ **[-]**	$(C_L/C_D)_{max}$ **[-]**	α - $(C_L/C_D)_{max}$ **[deg]**	ϕ
NACA0015	1.22	16.00	27.71	63.74	8.50	-1.13

In Figure 6a, the comparison of the formats of the test profile 10A and NACA0015 is showed. Note that profile 10A has the leading edge of greater thickness up to about the initial 40% of the chord and the trailing edge of slightly greater thickness in the final 25% of the chord.

In Figure 6b can be seen the comparison of the formats of the test profile 10I and NACA0015. Note the 10I profile has a leading edge of greater thickness up to the initial 60% of the chord and similar thickness in the rest of the profile.

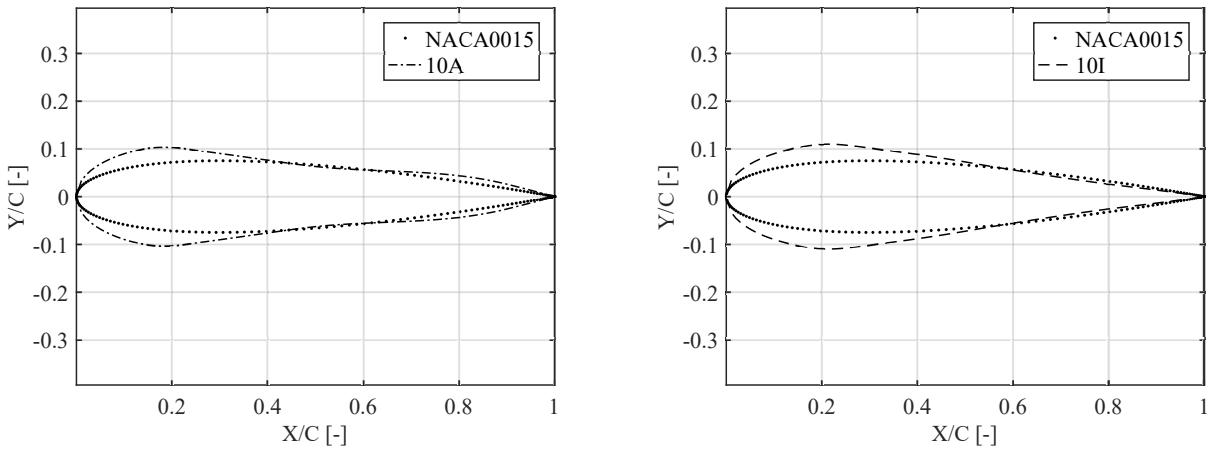

(a) Shape comparation between NACA0015 and test 10A. (b) Shape comparation between NACA0015 and test 10I.

Figure 6: Shape comparation profiles NACA015, 10A and 10I.

In Figure 7a, it is possible to see the comparison of the 15L and 15O and NACA0015 test profile formats. Note that the profile 15L-15O has the leading edge of greater thickness up to about the initial 30% of the chord. In the transition from the leading edge to the trailing edge the thickness is less. In the final 20% of the chord the thickness is similar.

In Figure 7b, the comparison of C_D graphics for all profiles is illustrated. It should be noted that the NACA0015 profile has a mild rising behavior in relation to the others. The higher the $(C_L)_{max}$, the greater the angle of attack in which the transition from asymptotic behavior to an abrupt growth of C_D occurs. This change occurs around the angle of $(C_L)_{max}$. You can also see the direct relationship between C_L and C_D.

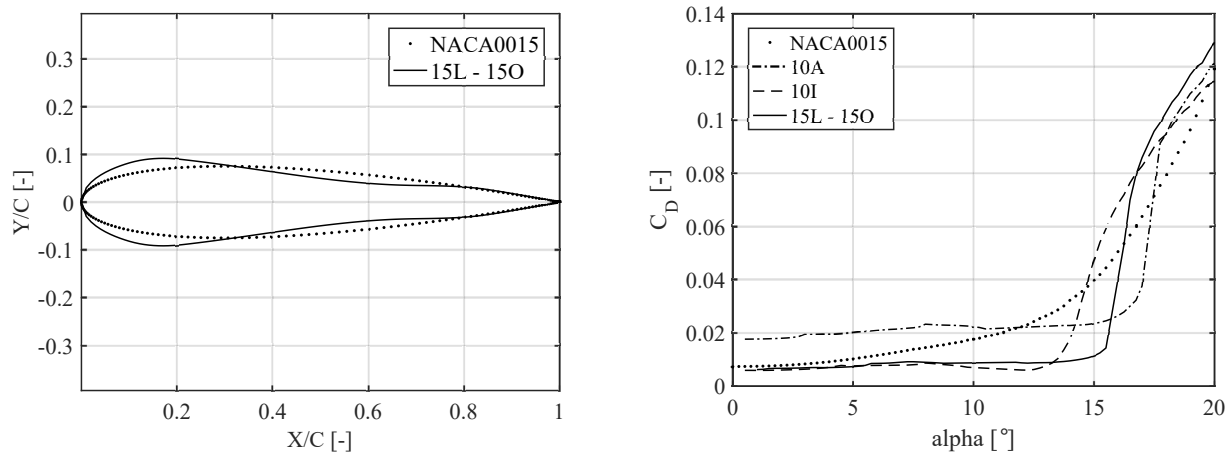

(a) Shape comparation between NACA0015 and tests 15L-15O.

(b) CD comparation.

Figure 7: Shape comparation profiles NACA015, 15L-15O and C_D.

In Figure 8a is presented the behavior of the lift coefficient as a function of the angle of attack of the profiles. The NACA0015 chart develops without any abrupt changes. The shape of the curves of the other profiles is similar, and they are apparently offset according to the $(C_L)_{max}$ of each one. Once again, the direct relationship between lift and drag is observed. In the comparison of lift/drag efficiency, in Fig. 8b, there is a tendency for the maximum to occur at greater angles when $(C_L)_{max}$ is greater except in the case of NACA0015. There is an inverse relationship between $(C_L)_{max}$ and efficiency at this point of operation $(C_L/C_D) - (C_L)_{max}$.

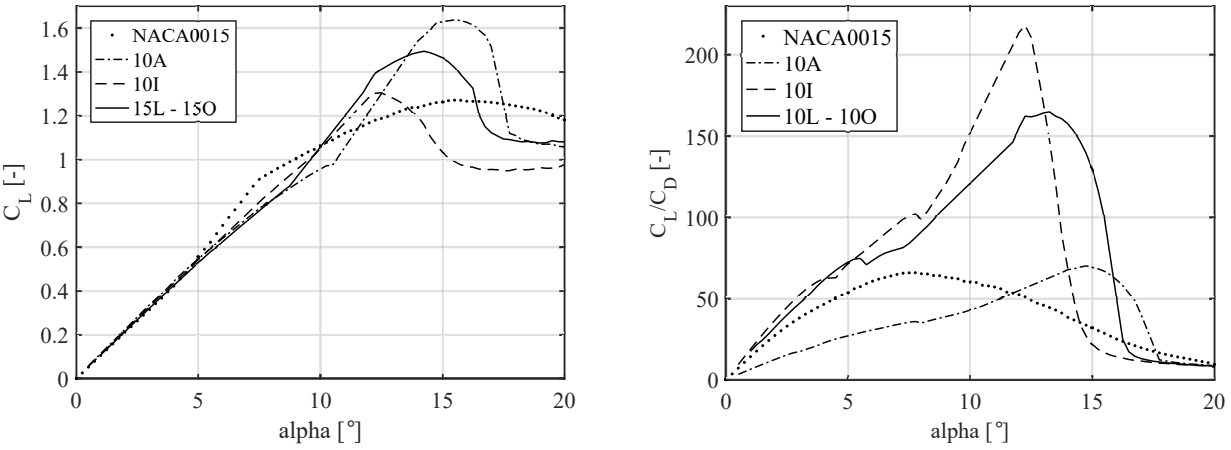

(a) CL comparation.

(b) CL/CD comparation.

Figure 8: Behaviour of C_L and C_L/C_D.

3.4 Cavitation verification

For cavitation verification is necessary evaluate σ from Eq. 1 with the values from Tab. 6 and compare with the negative of minimum C_P of each profile. The value is $\sigma = 54.7175$ and the C_p graphs are shown in Figures 9 and 10.

Table 6: Values for cavitation verification.

P_{atm} $[N/m^2]$	ρ [-]	P_v at $15°C$ $[N/m^2]$	v $[m/s]$	g $[m/s^2]$	h $[m]$
1.01325×10^5	10^3	1.7×10^3	2	9.81	1

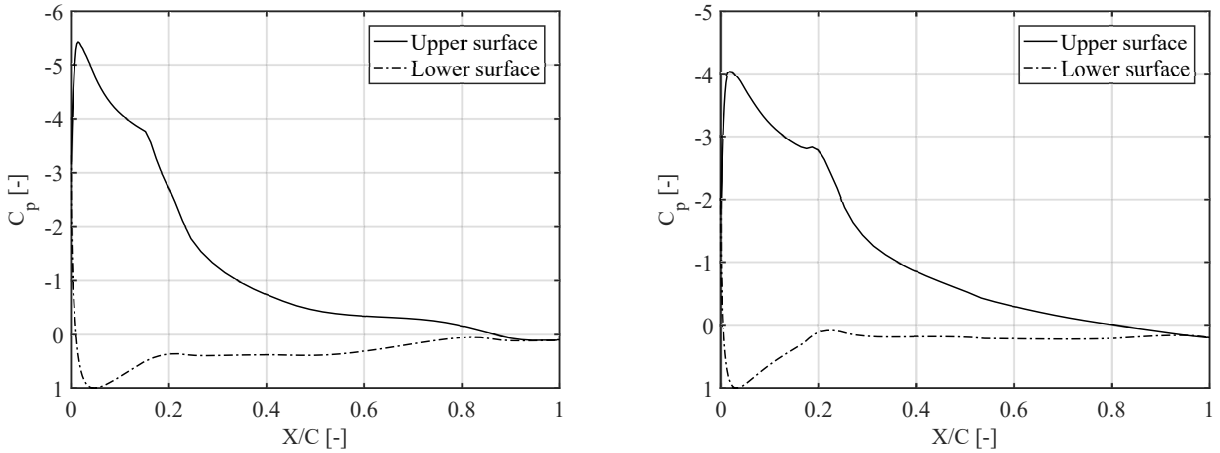

(a) Cp of test 10A at 15.50 degrees. (b) Cp of test 10I at 12.50 degrees.

Figure 9: Cp of test 10A and test 10I .

All values of negative C_p are much lower than the σ critical point. and for greater depths the occurrence of cavitation is further away. then, no adaptation is necessary.

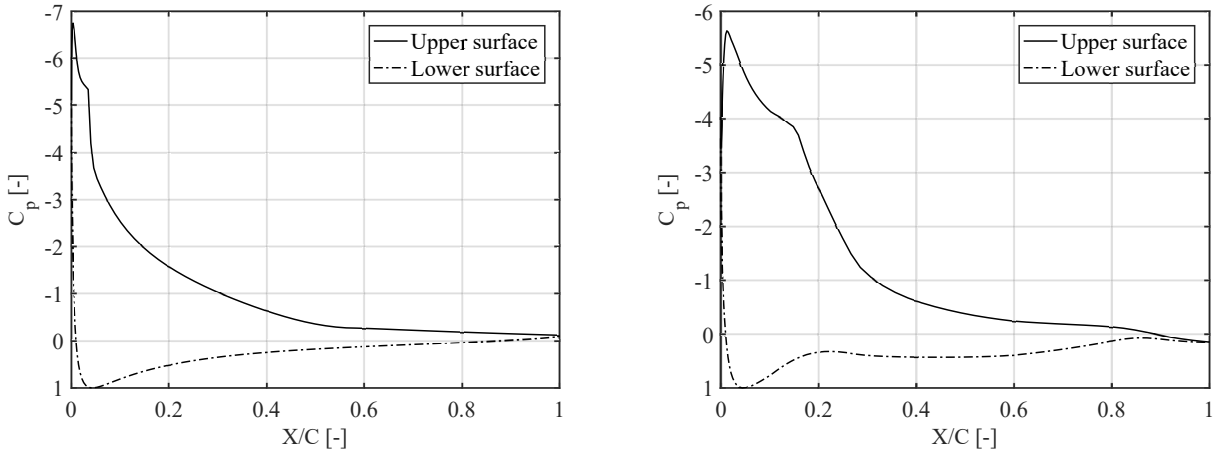

(a) Cp of NACA0015 at 16 degrees. (b) Cp of tests 15L and 15O at 12.50 degrees.

Figure 10: Cp of tests NACA0015, 15L and test 15O .

4. CONCLUSION

In the article, the genetic algorithm method was used to optimize hydrodynamic profiles used in cases of oscillating hydrofoils. The proposal was to use part the leading and trailing edges of different profiles, and thus, finding a profile mutation that would obtain better results for the lift coefficient and the lift-to-drag ratio.

The isolated optimization of $(C_L)_{max}$ showed in test 10A the improvement of approximately 34% in this parameter and 141% in the C_L/C_D efficiency compared to the NACA0015 currently used. The maximum number of generations for the test to achieve individual convergence is 8, suggesting the total generation is higher for the test to develop fully.

The individual optimization of $(C_L/C_D)-(C_L)_{max}$ showed an improvement of approximately 660% in this parameter and 7% in the parameter $(C_L)_{max}$ compared to the NACA0015 currently used. The maximum number of generations for the test to achieve individual convergence is 14, suggesting that the total generation is higher for the test to develop fully.

The multiobjective agglutination optimization presented two identical tests with the best parameter ϕ and an improvement of 452 % in efficiency $(C_L/C_D) - (C_L)_{max}$ and 22% in lift $(C_L)_{max}$. For the test to reach convergence, it must have at least 13 generations. When comparing the average of the parameters ϕ of each type of optimization with the others, it is noted that the optimization C_L and C_L/C_D had similar performances, while the agglutination obtained the best performance. Even so, the 10I test was configured as an outlier because it is the most suitable test application with the best ϕ indicator.

No adaptation in the flow regime or in the profiles is necessary because its point of operation was far from the occurrence of cavitation. All 45 tests proved to be better than NACA0015 and the 10I test is the most suitable for the proposed

application when considering the lift and the lift-to-drag efficiency at the same time.

5. REFERENCES

Abbott, I.H. and Von Doenhoff, A.E., 2012. *Theory of wing sections: including a summary of airfoil data*. Courier Corporation.

Anitha, D., Shamili, G., Kumar, P.R. and Vihar, R.S., 2018. "Air foil shape optimization using cfd and parametrization methods". *Materials Today: Proceedings*, Vol. 5, No. 2, pp. 5364–5373.

Bahaj, A., Molland, A., Chaplin, J. and Batten, W., 2007. "Power and thrust measurements of marine current turbines under various hydrodynamic flow conditions in a cavitation tunnel and a towing tank". *Renewable energy*, Vol. 32, No. 3, pp. 407–426.

Batten, W., Bahaj, A., Molland, A. and Chaplin, J., 2006. "Hydrodynamics of marine current turbines". *Renewable energy*, Vol. 31, No. 2, pp. 249–256.

Campos, G.A.P., 2013. *Study on mechanism applied power generation from ocean currents*. Master's thesis, Federal University of Rio de Janeiro, Rio de Janeiro, Brazil.

Campos, G.A.P., Raptopoulos, L.S.C. and Dutra, M.S., 2019. "Mathematical model for flapping foil". In *Proceedings of the 25nd International Congress of Mechanical Engineering - COBEM 2019*. Uberlândia, Brazil.

De Boor, C., De Boor, C., Mathématicien, E.U., De Boor, C. and De Boor, C., 1978. *A practical guide to splines*, Vol. 27. springer-verlag New York.

Della Vecchia, P., Daniele, E. and D'Amato, E., 2014. "An airfoil shape optimization technique coupling parsec parameterization and evolutionary algorithm". *Aerospace Science and Technology*, Vol. 32, No. 1, pp. 103–110.

Drela, M., 1989. "Xfoil: An analysis and design system for low reynolds number airfoils". In *Low Reynolds number aerodynamics*, Springer, pp. 1–12.

Drela, M. and Youngren, H., 2001. "Xfoil 6.9 user primer". Available at `https://web.mit.edu/drela/Public/web/xfoil/xfoil_doc.txt` (2020/07/30).

Elghali, S.B., Benbouzid, M. and Charpentier, J.F., 2007. "Marine tidal current electric power generation technology: State of the art and current status". In *2007 IEEE International Electric Machines & Drives Conference*. IEEE, Vol. 2, pp. 1407–1412.

Gaden, D.L., 2007. *An investigation of river kinetic turbines: performance enhancements, turbine modelling techniques, and an assessment of turbulence models*. Master's thesis, University of Manitoba, Winnipeg, Manitoba, Canada.

Goundar, J.N. and Ahmed, M.R., 2013. "Design of a horizontal axis tidal current turbine". *Applied energy*, Vol. 111, pp. 161–174.

Karbasian, H., Esfahani, J. and Barati, E., 2016. "The power extraction by flapping foil hydrokinetic turbine in swing arm mode". *Renewable Energy*, Vol. 88, pp. 130–142.

Marco, N. and Lanteri, S., 2000. "A two-level parallelization strategy for genetic algorithms applied to optimum shape design". *Parallel Computing*, Vol. 26, No. 4, pp. 377–397.

Mukesh, R., Lingadurai, K. and Selvakumar, U., 2014. "Airfoil shape optimization using non-traditional optimization technique and its validation". *Journal of King Saud University-Engineering Sciences*, Vol. 26, No. 2, pp. 191–197.

Quagliarella, D. and Cioppa, A.D., 1995. "Genetic algorithms applied to the aerodynamic design of transonic airfoils". *Journal of Aircraft*, Vol. 32, No. 4, pp. 889–891.

Silva, P., Shinomiya, L.D., de Oliveira, T.F., Vaz, J.R.P., Mesquita, A.L.A. and Junior, A., 2015. "Design of hydrokinetic turbine blades considering cavitation". In *The 7th International Conference on Applied Energy–ICAE2015, Energy Procedia*. Vol. 75, pp. 277–282.

Song, W. and Keane, A., 2004. "A study of shape parameterisation methods for airfoil optimisation". In *10th AIAA/ISSMO multidisciplinary analysis and optimization conference*. p. 4482.

Sørensen, B., 1991. "A history of renewable energy technology". *Energy policy*, Vol. 19, No. 1, pp. 8–12.

Tahani, M., Babayan, N., Astaraei, F.R. and Moghadam, A., 2015. "Multi objective optimization of horizontal axis tidal current turbines, using meta heuristics algorithms". *Energy Conversion and Management*, Vol. 103, pp. 487–498.

Wang, J., Periaux, J. and Sefrioui, M., 2002. "Parallel evolutionary algorithms for optimization problems in aerospace engineering". *Journal of Computational and Applied Mathematics*, Vol. 149, No. 1, pp. 155–169.

Wang, X., Song, B., Wang, P. and Sun, C., 2018. "Hydrofoil optimization of underwater glider using free-form deformation and surrogate-based optimization". *International Journal of Naval Architecture and Ocean Engineering*, Vol. 10, No. 6, pp. 730–740.

Zeng, Z.b. and Kuiper, G., 2012. "Blade section design of marine propellers with maximum cavitation inception speed". *Journal of Hydrodynamics, Ser. B*, Vol. 24, No. 1, pp. 65–75.

6. RESPONSIBILITY NOTICE

The authors are solely responsible for the printed material included in this paper.